Electrochimica Acta 71 (2012) 73–81

Contents lists available at SciVerse ScienceDirect

Electrochimica Acta

journal homepage: www.elsevier.com/locate/electacta

Glassy carbon electrodes modified with a dispersion of multi-wall carbon nanotubes in dopamine-functionalized polyethylenimine: Characterization and analytical applications for nicotinamide adenine dinucleotide quantification

Aurélien Gasnier[a], M. Laura Pedano[a], Fabiana Gutierrez[a], Pierre Labbé[b], Gustavo A. Rivas[a,*], María D. Rubianes[a,*]

[a] INFIQC, Departamento de Físico Química, Facultad de Ciencias Químicas, Universidad Nacional de Córdoba, Ciudad Universitaria, 5000 Córdoba, Argentina
[b] Département de Chimie Moléculaire, Université Joseph. Fourier, 38041 Grenoble Cedex 9, France

ARTICLE INFO

Article history:
Received 5 August 2011
Received in revised form 7 March 2012
Accepted 18 March 2012
Available online 5 April 2012

Keywords:
Carbon nanotubes functionalization
Electrochemical sensor
Polyethylenimine
Dopamine
NADH

ABSTRACT

We report the characterization of a dispersion of multi-wall carbon nanotubes (CNT) in a solution of polyethylenimine (PEI) functionalized with dopamine (Do), the electrochemical behavior of glassy carbon electrodes (GCE) modified with the resulting dispersion, and its analytical application for the highly sensitive quantification of NADH without fouling of the surface. The dispersion was obtained by sonicating for 60 min 1.0 mg CNT in 1.0 mL of 1.0 mg/mL PEI-Do solution prepared in 50/50 (v/v) ethanol/water. The presence of Do covalently bonded to PEI promotes hydrophobic π interactions with the CNT walls and improves significantly the dispersability of CNT in this mixture. The dispersion is highly stable since after 2 months resting at room temperature no phase separation was observed. This dispersion was drop-coated over GCE, and after solvent evaporation, a very reproducible and uniform coverage was obtained. An electrochemical pretreatment (activation) of such a modified GCE electrode allowed the sensitive quantification of NADH at potentials as low as −0.025 V. The response of NADH at the electrochemically activated GCE modified with the dispersion of CNT in PEI-Do solution (GCE/CNT-PEI-Do), demonstrated to be highly reproducible. The R.S.D. for the NADH sensitivity obtained with 15 electrodes and 3 different dispersions was 8.9%. Even more important, after 10 calibrations for NADH with the same surface the decrease in the sensitivity was smaller than 10%. The dispersion was characterized by Field Emission Scanning Electron Microscopy (FE-SEM), Fourier Transform Infrared Spectroscopy (FT-IR) while the electrodes modified with the dispersion were evaluated using different electrochemical techniques (Cyclic voltammetry (CV), Amperometry and Electrochemical Impedance Spectroscopy (EIS)).

1. Introduction

The electrochemical quantification of reduced nicotinamide adenine dinucleotide (NADH) through its oxidation to NAD^+ has received considerable attention since it is an essential biological molecule found in all living cells that participates as coenzyme in many important redox reactions catalyzed by dehygrogenases [1]. However, the direct electrochemical oxidation of NADH is highly irreversible with an elevated overpotential at common electrodes. The oxidation products of NADH can be adsorbed on the electrode surface producing passivation of the electrode and, consequently, poor sensitivity, poor selectivity and unstable analytical signals [1]. Thus, one of the main challenges to sense NADH electrochemically is to find a surface that avoids all these problems.

The functionalization of electrodes by using redox-active species may sustain electrocatalytic processes granting an enhanced reactivity towards a given analyte, and in some cases, a poor reactivity towards species considered as interferents, improving in this way the efficiency/selectivity of electroanalytical methodologies [1–5]. In that aspect, Rubianes and Strumia [6] have reported the catalytic activity on NADH electrooxidation of a GCE modified with polyethylenimine (PEI) covalently functionalized with the catecholamine dopamine (Do).

Carbon nanotubes (CNT) have been also used to successfully modify electrodes due to their intrinsic electrocatalytic properties. The resulting electrodes have demonstrated to be an excellent alternative in terms of surface and reactivity enhancement [7–9]. Despite their unique electrocatalytic properties, CNT tend to aggregate in aqueous solutions due to strong π–π interactions between their aromatic rings [10,11], making difficult their dispersion. To overcome their aggregation and take profit of their full capabilities, CNT have been generally dispersed in aqueous media by wrapping

* Corresponding authors. Tel.: +54 351 4334169/80; fax: +54 351 4334188.
E-mail address: rubianes@fcq.unc.edu.ar (M.D. Rubianes).

0013-4686/$ – see front matter © 2012 Elsevier Ltd. All rights reserved.
doi:10.1016/j.electacta.2012.03.073

with different polymers. Nafion [12], chitosan [13,14], polylysine [15,16], PDDA [17], polyacrylic acid [18,19], and hialuronic acid [20] among other polymers, have been successfully used as dispersing agents. Our group has previously reported the successful dispersion of CNT with PEI [21], which wraps the nanotubes, making their environment more hydrophilic and favoring their dispersion. Glassy carbon electrodes (GCE) modified with this dispersion have been used for the efficient quantification of bioanalytes either in batch [21,22] or in flow involving Flow Injection Analysis and Capillary Electrophoresis [23]. Aromatic molecules such as pyrene [24], methylene blue [25] and imidazolium-containing ionic liquids [26] have been employed to functionalize CNT through strong $\pi-\pi$ stacking interactions. Those aromatic systems are very similar from the electronic point of view to graphite and can be seen as a cut piece from a graphite sheet; therefore, the interaction between two CNT or the different layers of a multi-walled carbon nanotubes or between the aromatic molecules and CNT is quite similar [24–27]. Nevertheless, there are rare examples of electrodes modified by both CNT and polymers modified with aromatic redox-active species [28].

In this work we report the dispersion of CNT in PEI functionalized with dopamine (PEI-Do) to obtain: (a) a dispersing agent for CNT that confers more stability to the dispersion and its deposit on GCE, (b) a redox-active polymer that allows to follow by electrochemical techniques the modification of CNT through the redox signal of Do, and (c) the precursor (Do) of the mediator that catalyzes the electrochemical reaction of NADH immobilized in the same dispersing agent.

In the following sections we present: (i) The characterization of the CNT-PEI-Do dispersion before and after deposition on the electrode surface using different techniques: Field Emission Scanning Electron Microscopy (FE-SEM), Fourier Transformed Infrared Spectroscopy (FTIR), Cyclic voltammetry (CV), Electrochemical Impedance Spectroscopy (EIS) and Amperometry; (ii) A comparison of the electrochemical behavior of bare GCE and GCE modified with different polymers or CNT dispersions: GCE/PEI, GCE/PEI-Do, GCE/CNT, GCE/CNT-PEI, and GCE/CNT-PEI-Do, either in buffer solution or in the presence of NADH; and (iii) The analytical performance of GCE/CNT-PEI-Do for the amperometric quantification of NADH.

2. Experimental

2.1. Reagents

Polyethylenimine (M_w 750 kDa, catalog number P-3143), dopamine, NADH and glutaraldehyde (reagent grade) were purchased from Sigma and used without further purification. Multi-walled carbon nanotubes powder (95% purity (30 ± 15) nm diameter, (1–5) microns length), were obtained from NanoLab, Inc. (MA, USA) and used as received.

A 0.050 M phosphate buffer solution pH 7.40 was employed as supporting electrolyte, except stated otherwise. Ultrapure water (resistivity = 18 MΩ cm) from a Millipore-MilliQ system was used for preparing all the solutions.

2.2. Apparatus

Electrochemical experiments were performed with Epsilon (BAS) and TEQ_04 potentiostats. The electrodes were inserted into the cell (BAS, Model MF-1084) through holes in its Teflon cover. Glassy carbon electrodes from CH-instruments (3 mm diameter) were used as working electrodes. A platinum wire and Ag/AgCl, 3 M KCl (BAS, Model RE-5B) were used as counter and reference electrodes, respectively. All potentials are referred to the latter. A magnetic stirrer provided the convective transport during amperometric measurements, with the agitation speed set at 800 rotations per minute. An ultrasonic bath Testlab 160 W was used to prepare the CNT dispersions.

Electrochemical Impedance Spectroscopy measurements were performed with a Solartron 1287 FRA 1260. The impedance spectra were analyzed by using the Z-view program.

UV–vis experiments were performed with a UV-1700 Pharma Spec Shimadzu spectrophotometer. IR spectra were recorded using a FTIR instrument (Bruker IFS 28) by drop-coating and drying the samples on a ZnSe disk. Scanning Electron Microscopy (SEM) images were obtained with a Field Emission Gun Scanning Electron Microscope (Zeiss, $\sum$IGMA model). The dispersions were previously drop-coated and air dried over GCE discs.

2.3. Synthesis and quantification of PEI functionalized with dopamine (PEI-Do)

Synthesis, purification and characterization of PEI-Do were performed as described by Rubianes and Strumia [6]. Briefly, the covalent attachment of Do was performed through imination of the amino groups of PEI with glutaraldehyde. The covalent attachment of Do to PEI was confirmed from the presence of the imine bands at 1630 cm^{-1} by IR spectroscopy (Section 3.1.3). The resulting PEI-Do was purified using a Sephadex G-10 column of 18 cm length and 1.3 cm width. Milli Q water was used as elution solvent. After elution of the dead volume, the first fraction presented the highest Do concentration covalently bond to PEI (obtained from the absorbance at 280 nm, results not shown). The modified polymer was readily separated from unbounded Do since the fractions 5–7 presented a clear absorption peak of Do at 280 nm. This purification protocol was repeated on the complete crude sample and, after UV–vis characterization, the first fractions were combined. A portion of these combined fractions was evaporated to dryness and the mass concentration was 4.5 g/L. The amount of Do immobilized at the polymer was 10% (w/w). This amount was determined by UV–vis spectroscopy from the band at 280 nm, and by amperometry at 300 mV (potential that corresponds to Do oxidation peak potential at GCE), from the corresponding calibration curves with pure Do (not shown).

2.4. Preparation of dispersions and modified electrodes

PEI and PEI-Do solutions were prepared at 1.0 mg/mL in a 50:50 (v/v) ethanol/water media. CNT, CNT-PEI-Do and CNT-PEI dispersions were obtained by mixing 1.0 mg of CNT with 1.0 mL of the corresponding solution (50:50 (v/v) ethanol/water, 1.0 mg/mL PEI-Do, or PEI, respectively) followed by 60 min sonication.

Previous to their modification, GCEs were consecutively polished with alumina slurries of 1.0, 0.30 and 0.05 μm for 2 min each, and then cycled 10 times in a 0.050 M phosphate buffer solution pH 7.40 from −0.200 to +0.800 V to obtain a stable profile.

The different tested modified electrodes (GCE/CNT-PEI-Do, GCE/CNT-PEI, GCE/CNT, GCE/PEI-Do, or GCE/PEI) were prepared by a simple casting method: the polished GCE were modified by drop-coating with 20 μL of CNT-PEI-Do, CNT-PEI, CNT, PEI-Do, or PEI dispersion/solution. The solvent was evaporated in air for 90 min.

2.5. Procedure

For the electrochemical measurements, 0.050 M phosphate buffer solution pH 7.40 was used as supporting electrolyte. Cyclic voltammetry experiments were performed at 0.010 V s^{-1}. The amperometric experiments were carried out at −0.025 V or by applying the desired potential and allowing the transient current to reach a steady-state value prior to the addition of the analyte

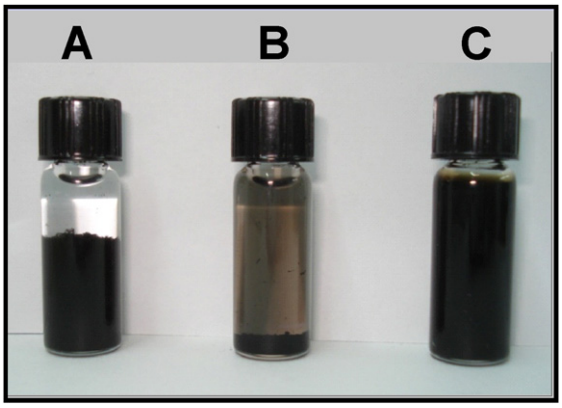

Fig. 1. Pictures for dispersions of CNT (A), CNT-PEI (B) and CNT-PEI-Do (C) in ethanol/H_2O (50:50, v/v), prepared by 60 min sonication and allowed to rest for 60 days.

and the subsequent current monitoring. All the experiments were conducted at room temperature.

The EIS experiments were performed between 1.0×10^5 Hz and 1.0×10^{-2} Hz, with a potential perturbation of 10 mV and a working potential of −0.025 V in a 0.050 M phosphate buffer solution pH 7.40, in the absence and presence of 1.0×10^{-3} M NADH.

3. Results and discussion

3.1. Characterization of CNT-PEI-Do dispersions

3.1.1. Macroscopic observations

Fig. 1 shows pictures of vials containing 1.0 mg/mL CNT dispersed in ethanol–water 50/50 (v/v): (A) in the absence of any polymer, (B) in the presence of 1.0 mg/mL PEI and (C) 1.0 mg/mL PEI-Do after 60 min initial sonication and further 60 days repose at room temperature. It is evident that the sonication in ethanol/water can not eliminate the bundles of CNT that are aggregated and settled down at the bottom of the vial (A). On the contrary, the sonication of CNT in the presence of PEI (B) decreases the number of aggregates and facilitates the dispersion although some bundles still remains and settle down. Interestingly, when sonicating CNT in the presence of PEI-Do (C), CNT dispersion looks even more homogeneous than with PEI, and do not settle down still after 60 days. Even after prolonged centrifugation a very dark aqueous phase was observed. The $\pi-\pi$ interaction between the aromatic region of Do attached to PEI and the hydrophobic side wall of CNT [24–27] promotes a better wrapping of the polymer around the CNT, enabling them to disperse more readily in water. The surface of the wrapped nanostructures becomes more hydrophilic owing to the amine groups present in the PEI, improving, thus, the quality of the dispersion. These results are a clear evidence of the high physical stability of the CNT-PEI-Do dispersion even after 2 months at room temperature.

3.1.2. SEM characterization

Fig. 2 displays SEM images of glassy carbon surfaces covered with 1.0 mg/mL CNT dispersed in (A) 50/50 (v/v) ethanol/water, (B) 1.0 mg/mL of PEI in ethanol/water and (C) 1.0 mg/mL PEI-Do in ethanol/water. When GCE is modified with the dispersion of CNT in ethanol/water, the surface is completely covered by CNT, although the coverage is unsymmetrical as it is more clearly shown in the inset (Fig. 2A). When the dispersion is performed in the presence of PEI, the glassy carbon surface shows a complete coverage although it presents different density of CNT (*inset* in Fig. 2B). The addition of PEI-Do to the dispersing solvent produces a very uniform and homogeneous distribution of the deposit over the complete surface of the electrode, with a reproducible circle shape, in opposition

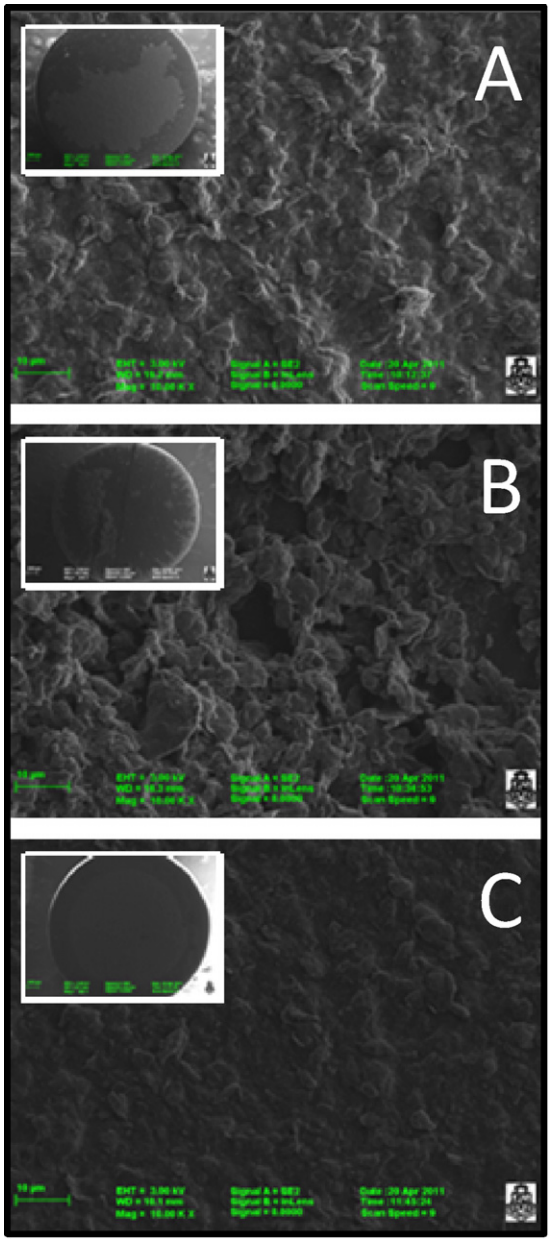

Fig. 2. SEM images of glassy carbon disks covered with 1.0 mg/mL CNT dispersed in (A) 50/50 (v/v) ethanol/water, (B) 1.0 mg/mL of PEI in ethanol/water and (C) 1.0 mg/mL PEI-Do in ethanol/water. Magnification: 10,000×, scale bare 10 μm. *Inset*: lower magnification (250×) of the given surface.

to what is observed for CNT/PEI dispersion (Fig. 2C). Nevertheless, when the glassy carbon disks were modified with CNT-PEI-Do, the size of the domains seems to increase, showing less marked boundaries and a flattened and more homogeneous topography. Thus, the presence of Do functionality in the polymer is decisive to ensure a complete coverage of the GCE surface.

3.1.3. IR characterization

Fig. 3 displays IR spectra for Do (a), PEI (b), PEI-Do (c) and CNT dispersed in PEI-Do (d). The Do spectrum (Fig. 3a) shows characteristic absorption bands of the aromatic compounds: vibrations due to C—H bonds appear at 900 and 675 cm^{-1} (out of plane) and between 1300 and 1000 cm^{-1} (in plane), skeletal vibration that involve C–C stretching between 1600 and 1400 cm^{-1} and the combination and overtones bands in the 2000–1650 cm^{-1} region. The spectrum of PEI (Fig. 3b) presents wider peaks, consistently with its

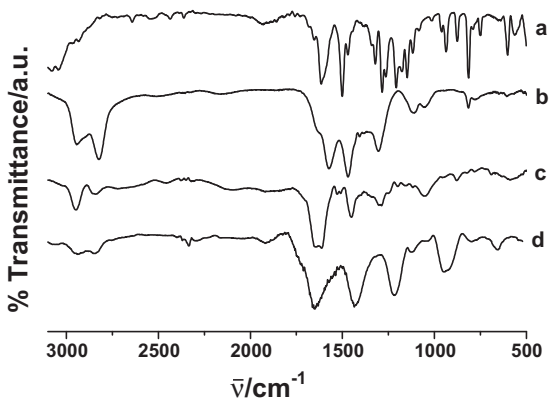

Fig. 3. FTIR spectra for (a) Do, (b) PEI, (c) PEI functionalized with dopamine, (d) CNT functionalized with PEI-Do.

polymeric nature. Peaks at 1575 and 1466 cm^{-1} correspond to the bending vibration of N–H, and those at 1306, 1110 and 1050 cm^{-1} to the stretching vibration of C–N of primary and secondary amines. Absorption peaks at 2946 cm^{-1} and 2830 cm^{-1} can be assigned to aliphatic C–H stretching frequencies of the ethylene group of PEI. The spectrum corresponding to PEI-Do (Fig. 3c) presents a broad and important band centered at 1630 cm^{-1} that indicates the formation of the imine linkage, confirming the reaction of glutaraldehyde with the NH_2 residues of PEI and Do. The spectrum corresponding to CNT dispersed in PEI (not shown) presented the peaks due to the presence of basic nitrogen-containing groups of PEI previously indicated (1575 and 1466 cm^{-1}), corroborating that PEI is effectively wrapped on the CNT walls upon ultrasonication, and that since those nitrogenated groups are hydrophilic, they facilitate the dispersion of CNT in aqueous medium. The spectrum of CNT-PEI-Do (Fig. 3d) displays some characteristic bands common to the spectra of CNT-PEI (not shown) and PEI-Do (Fig. 3c) in the region between 1300 and 1700 cm^{-1}, and to that of Do (Fig. 3a) between 900 and 1300 cm^{-1}. It is important to note that the spectrum of a previously washed sediment of the CNT-PEI-Do dispersion obtained after centrifugation (not shown), presented bands in the Do characteristic region which remained even after extensive washing, demonstrating a strong interaction between the aromatic ring of Do and the CNT walls. These results confirm the effective and stable functionalization of CNT with PEI-Do, which on one hand provides a strong CNT–polymer interaction through the Do moieties, and on the other hand facilitates CNT–polymer–solvent interactions through the hydrophilic amine groups of the polymer backbone.

3.1.4. Electrochemical characterization

In order to perform a rational design of an electrochemical sensor for NADH using GCE/CNT-PEI-Do, it is necessary to know the response of NADH at GCE modified with the different constituents of the proposed dispersion. Fig. 4 shows the voltammetric response of six different electrodes, three without CNT: (A) GCE, (B) GCE/PEI, (C) GCE/PEI-Do, and three with CNT: (D) GCE/CNT, E) GCE/CNT-PEI, F) GCE/CNT-PEI-Do. The voltammograms were obtained in a 0.050 M phosphate buffer solution pH 7.40 without (dashed lines) and with (solid line) 2.0 mM NADH.

To facilitate the comprehension of the electrochemical performance of the different platforms, we will first describe their behavior in buffer solution (Fig. 4, dashed lines): (a) The current increase observed in B and E at potentials higher than 0.4 V is attributed to the oxidation of PEI amine groups [29]. The same explanation can be given to the wave observed at similar potentials in C and F. (b) The presence of CNT on the electrode surface (D–F) produces an important enhancement in the capacitive and faradaic currents due to the increment in the electroactive area and to the electroactivity of CNT. It is interesting to mention that the areas corresponding to the different surfaces, evaluated by chronopotentiometric experiments using hydroquinone as a redox probe, present the following order: GCE/CNT-PEI-Do > GCE/CNT-PEI > GCE/CNT > GCE (not shown). This order is in agreement with the macroscopic observation of the different dispersions and the SEM images of GCE-modified surfaces that show a more efficient dispersion of CNT in PEI-Do solution than in PEI solution or just ethanol/water. This improvement in the efficiency of the

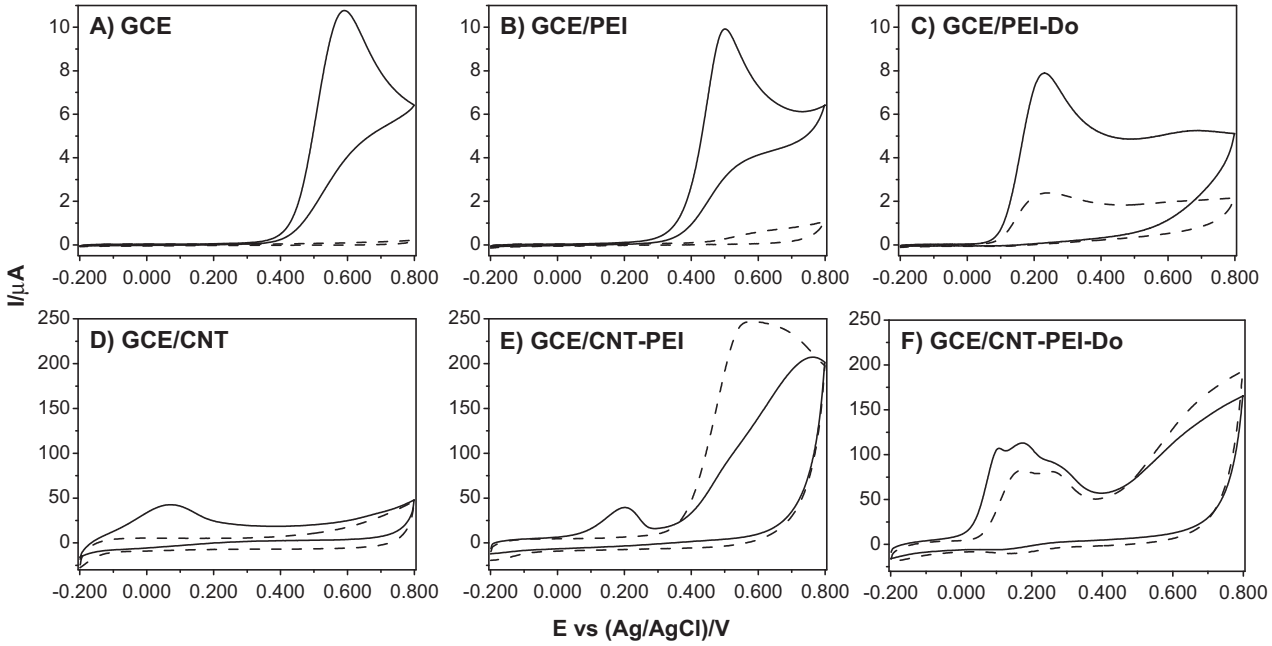

Fig. 4. Cyclic voltammograms obtained in 0.050 M phosphate buffer (dashed line) and 2.0 mM NADH (solid line) at (A) GCE, (B) GCE/PEI, (C) GCE/PEI-Do/, (D) GCE/CNT, (E) GCE/CNT-PEI, (F) GCE/CNT-PEI-Do. Scan rate: 10 mV/s.

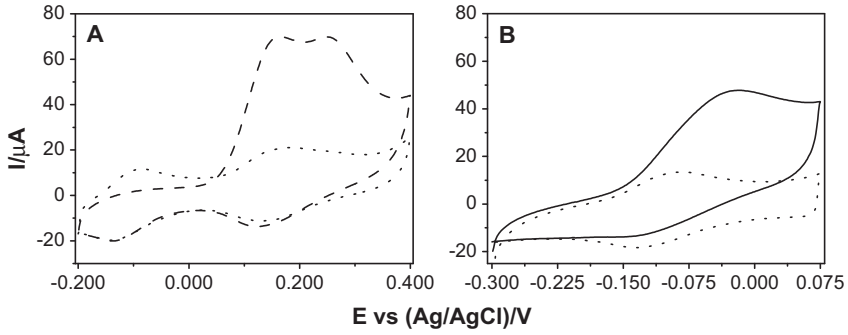

Fig. 5. Cyclic voltammograms obtained at GCE/CNT-PEI-Do. (A) First (dashed line) and second (dotted line) cycles in 0.050 M phosphate buffer pH 7.40. (B) Second cycle in buffer (dotted line) and in 2.0 mM NADH solution (solid line).

dispersion produces an increment in the density of CNTs at the electrode surface and, as a consequence of that, an increase in the electroactive area of GCE/CNT-PEI-Do. (c) At the GCE/PEI-Do (C), the peak observed in buffer solution at 0.240 V is attributed to the oxidation of Do attached to the polymer [6]. (d) When the GCE is modified with CNT-PEI-Do (F), two overlapped peaks appear at 0.170 and 0.260 V. These peaks can be attributed to the oxidation of two fractions of Do within the deposited dispersion that could differ either in their protonation state (charged vs. uncharged species), and/or entanglement within the dispersion (surface vs. bulk), and/or contact with the CNT (delocalized vs. isolated π-electrons).

In the presence of 2.0 mM NADH (Fig. 4, solid lines), the electrodes present the following features: (a) At the bare GCE (A) NADH electrooxidation occurs at highly positive potentials (0.590 V). (b) At the GCE/PEI (B) there is a small shifting of the NADH oxidation peak potential towards less positive values (0.500 V vs. 0.590 V) compared to GCE, indicating that PEI does not passivate the electrode surface at variance with other polymers. (c) The comparison of the oxidation signal of NADH (solid line) on the GCE/PEI (B) with that on the GCE/PEI-Do (C) reveals that the modification of the surface with Do shifts the oxidation peak of NADH to 0.230 V. This peak matches the oxidation potential of Do moieties already observed in buffer solution (C, dashed line) but is three times more intense in NADH solution (C, solid line). Thus, it can be assumed that the catalytic oxidation of NADH on this electrode is mediated by the oxidation product of Do (dopaminequinone) in agreement with the results previously reported [6]. This was confirmed by the observation of a current rise along with the increment in NADH concentration (not shown). (d) When incorporating CNT (GCE/CNT (D)), the oxidation of NADH occurs at a potential 520 mV less positive than at bare GCE (A) with a three-fold current increase, indicating an important electrocatalytic effect of CNT. (e) At the GCE/CNT-PEI (E), NADH is oxidized at a potential 130 mV more positive than at the GCE/CNT (D) and the peak current is smaller. These results indicate that, even when PEI does not passivate the electrode, its small physical blocking effect reduces the global catalytic activity of CNT. (f) At the GCE/CNT-PEI-Do (F), a new anodic peak at 0.100 V appears in NADH solution (solid line) with respect to the voltammetric response of the electrode in buffer solution (dashed line). Additional cyclic voltammetry experiments performed at different concentrations of NADH (0.10, 0.50, 1.0 and 2.0 mM) demonstrated that the peak at 0.100 V increases as the concentration of NADH increases, confirming that it is due to NADH oxidation (not shown). On this electrode the oxidation of NADH occurs 70 mV before the oxidation of Do moieties, implying that in the presence of carbon nanotubes, NADH might be oxidized before the dopaminequinone is formed, preventing it from any catalytic activity. In the following section we investigate the effect of forming dopaminequinone at the GCE/CNT-PEI-Do on the oxidation of NADH.

3.2. Influence of the pretreatment of the electrode

One of the goals in attaching Do to PEI was to generate species with catalytic activity. Considering that dopaminequinone, the oxidation product of Do, can be converted into dopaminechrome and that p-quinone-imines are catalytically active for the oxidation of NADH [30], we investigated the effect of the pre-oxidation of Do attached to the polymer on the electrochemical behavior of NADH.

Fig. 5A displays cyclic voltammograms obtained in a 0.050 M phosphate buffer solution pH 7.40 at GCE/CNT-PEI-Do between −0.200 V and 0.400 V, that is, at potentials where Do is completely oxidized. The first cycle (dashed line) shows two contributions in the anodic scan at 0.170 and 0.260 V, and a reduction peak at 0.120 V, in agreement with Fig. 4F. However, at variance with the voltammetric profile displayed in Fig. 4F, a second reduction peak appears at −0.150 V. In the second cycle (dotted line), this new peak gives rise to an additional reversible peak system with oxidation at −0.090 V. This peak system is obtained only if the anodic potential reaches 0.400 V but does not exceed this value, and it is attributed to the oxidation of the leucodopaminechrome formed as a consequence of the conversion of dopaminequinone into dopaminechrome [31]. When the potential is scanned up to 0.200 V, that is, before the definition of the second Do oxidation peak, the peaks at −0.090 V do not appear. The CVs obtained after performing similar pretreatment on the GCE, GCE/PEI, GCE/PEI-Do, and GCE/CNT-PEI did not exhibit the peaks system at −0.100 V, indicating that this process develops only when Do and CNT are simultaneously present at the electrode surface and the electrode is "activated" by scanning the potential up to 0.400 V. Herein, we will refer as "activation" to the process of performing a potential scan at a freshly prepared GCE/CNT-PEI-Do electrode in phosphate buffer from −0.200 V to 0.400 V at 0.010 V s^{-1}.

Fig. 5B shows the voltammetric profiles between −0.300 V and 0.075 V obtained at a GCE/CNT-PEI-Do previously "activated": in buffer (dotted line) and in 2.0 mM NADH solution (solid line). The voltammogram obtained in the presence of NADH, shows a large increase in the oxidation current at potentials higher than −0.090 V (solid line), while the associated reduction current significantly decreases with respect to the voltammogram obtained in buffer solution (dotted line). These results are a clear evidence of the catalytic oxidation of NADH: the compound generated during the activation of GCE/CNT-PEI-Do is oxidized at −0.090 V, then is chemically reduced in the presence of NADH, and reoxidized electrochemically, giving place to the catalytic wave at −0.040 V. In this way, the local concentration of this compound decreases and the

Table 1
Comparison of the parameters obtained from the electric circuit model (EC) and the Cole–Cole plots for the GCE/CNT-PEI-Do in absence and presence of 1.0×10^{-3} M NADH.

Sensing surface	C_a (F)	Γ (mol cm^{-2})
CNT-PEI-Do (EC)	$4.9 \times 10^{-4} \pm 0.4 \times 10^{-4}$	$1.7 \times 10^{-9} \pm 0.3 \times 10^{-9}$
CNT-PEI-Do (Cole–Cole)	$5.6 \times 10^{-4} \pm 0.7 \times 10^{-4}$	$1.9 \times 10^{-9} \pm 0.3 \times 10^{-9}$
CNT-PEI-Do/NADH (EC)	$4.8 \times 10^{-4} \pm 0.7 \times 10^{-4}$	$1.8 \times 10^{-9} \pm 0.3 \times 10^{-9}$
CNT-PEI-Do/NADH (Cole–Cole)	$4.5 \times 10^{-4} \pm 0.7 \times 10^{-4}$	$1.7 \times 10^{-9} \pm 0.3 \times 10^{-9}$

C_a = pseudocapacitance of surface-confined electroactive species. Γ = concentration of surface-confined electroactive species calculated from $\Gamma = 4RTC_a/F^2A$.

reduction wave at −0.150 V is less intense in the presence of NADH than in buffer.

3.3. Electrochemical impedance spectroscopy characterization of "activated" GCE/CNT-PEI-Do

EIS is a powerful method for characterizing the electrical interfacial properties and is a very sensitive technique to study surface-confined electroactive species. The impedance of the surface confined species is analyzed using a modified Randles circuit. The simplest model for surface-confined electroactive species includes contributions to the electrochemical response from three sources: uncompensated solution resistance (R_s), double layer film capacitance (C_{dl}), and faradaic activity of surface-confined electroactive species, which is represented by a charge-transfer resistance (R_{ct}) and a pseudocapacitance (C_a) (see *inset* Fig. 6). Therefore, C_a and R_{ct} values can be determined from the spectra fitting using the mentioned equivalent electrical circuit [32,33].

In the case of a surface confined redox system, the results can also be presented as Cole–Cole plots [32,33], where the data are shown in the $1/j\omega Z$ plane in the form of C_{im} versus C_{re} (where C_{Im} and C_{Re} are the imaginary and real parts of the interfacial complex capacitance, respectively, $j = (-1)^{1/2}$, and Z is the impedance). In the Cole–Cole plot, the data are shown in the $1/j\omega Z$ plane, rather than in the Z plane. In general, if the impedance of a system is given by:

$$Z = Z_{Re} - jZ_{Im} \tag{1}$$

The abscissa in Cole–Cole plot is:

$$Re\left(\frac{1}{j\omega Z}\right) = C_{Re} = \frac{Z_{Im}}{\omega(Z_{Re}^2 + Z_{Im}^2)} \tag{2}$$

While the ordinate is:

$$-Im\left(\frac{1}{j\omega Z}\right) = C_{Im} = \frac{Z_{Re}}{\omega(Z_{Re}^2 + Z_{Im}^2)} \tag{3}$$

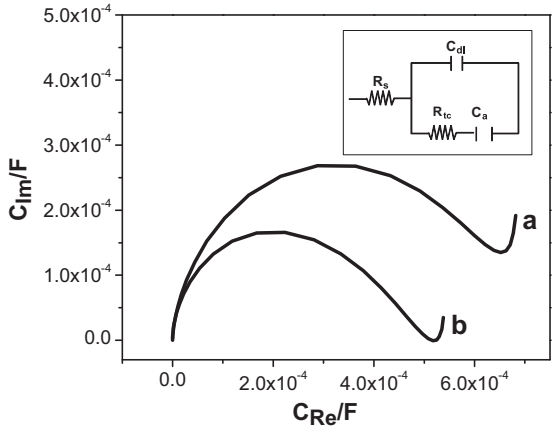

Fig. 6. Cole–Cole plots for GCE/CNT-PEI-Do obtained in the absence (a) and in the presence (b) of 1.0×10^{-3} M NADH in 0.050 M phosphate buffer solution pH 7.40. Frequency: between 1.0×10^5 Hz and 1.0×10^{-2} Hz; potential perturbation: 10 mV; working potential: −0.025 V. *Inset*: electric circuit model (EC) used.

where $j = (-1)^{1/2}$; $\omega = 2\pi f$; f is the frequency, and *Re* and *Im* represent the real and imaginary components, respectively.

Fig. 6 shows a comparison of the Cole–Cole plots for GCE modified with CNT-PEI-Do in the absence (a) and presence (b) of 1.0×10^{-3} M NADH in a 0.050 M phosphate buffer solution pH 7.40. From these plots, it is possible to obtain the surface concentration of redox species (Γ) (in moles per surface area) if the pseudocapacitance is known according to equation (4):

$$\Gamma = \frac{4RTC_a}{F^2A} \tag{4}$$

where R is the universal gas constant, T is the temperature, F is the Faraday constant, and A is the area of the electrode. C_a can be obtained both from the equivalent circuit and also from the maximum of the semicircle of the Cole–Cole plot. Table 1 shows the values of Γ and C_a determined from both methods: the electrical circuit fitting (EC) and the Cole–Cole plots. With both methods, the obtained C_a values are quite similar either in buffer or NADH solution. Additionally, the concentration (Γ) of the surface-confined redox species originated during the pretreatment of GCE/CNT-PEI-Do are similar either in the absence or presence of NADH, indicating that, as expected, the amount of immobilized redox species at the electrode surface is the same in both cases and does not depend on the presence of NADH, solely on its generation by the pretreatment activation of the electrode.

To confirm the importance of Do as precursor of the redox mediator electrogenerated during the potentiodynamic activation of GCE/CNT-PEI-Do and the catalytic effect of this mediator towards NADH oxidation, we compare the R_{ct} values obtained from Nyquist plots at −0.025 V for GCE/CNT-PEI and GCE/CNT-PEI-Do in 0.050 M phosphate buffer solution pH 7.40 in the absence and presence of 1.0×10^{-3} M NADH solution (not shown). The results obtained for GCE/CNT-PEI were fitted with an (R(RC)) circuit, while those obtained for GCE/CNT-PEI-Do, were fitted with the modified Randles circuit. In the case of GCE/CNT-PEI-Do the R_{ct} obtained in buffer solution was almost 1200 times smaller than the one obtained at GCE/CNT-PEI (2.32×10^2 Ω vs. 2.78×10^5 Ω) due to the presence of the oxidation product of dopamine generated during the activation of the electrode. In the presence of NADH, the R_{ct} value for

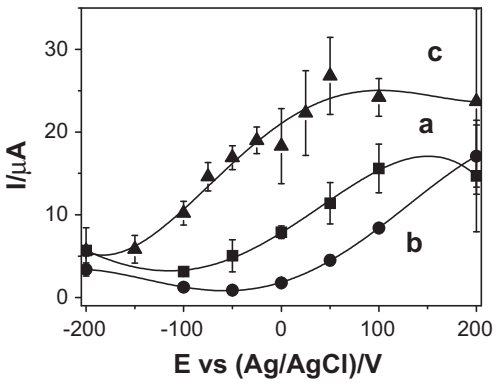

Fig. 7. Hydrodynamic voltammograms for 1.0 mM NADH at GCE/CNT (a, ■), GCE/CNT-PEI (b, ●) and GCE/CNT-PEI-Do(c, ▲).

Table 2
Comparison of the analytical performance of several amperometric sensors for NADH quantification.

Sensing surface	*E* vs. (Ag/AgCl) (V)	Linear range (mol dm^{-3})	Sensitivity (μA dm^3 mol^{-1})	DL (μmol dm^{-3})	RSD	Stability	Ref
Poly-6-vinyl coenzyme Q_0/GCE	0.425	1.0×10^{-5}–1.0×10^{-4}	3.3×10^{5s}*	NR	NR	NR	[36]
Poly-hematoxylin/GCE	0.300	1.0×10^{-7}–1.5×10^{-4}	NR	NR	2.2% (n = 6)		[37]
Cyt C:DOPE + UQ_{10}/poly-TTCA/AuNP/SPCE	0.175	1.0×10^{-6}–5.0×10^{-3}	0.851	500	2.6% (n = 5)	90%–1 month 4 °C	[38]
NADoxidase-Fc/SPCE	0.25	5.0×10^{-4}–3.8×10^{-3}	1.423×10^4	High	NR	NR	[39]
PEDOTSDS–AgNP–MB/GCE	−0.050	1.0×10^{-5}–5.6×10^{-4}	2×10^3	0.1	NR	NR	[40]
branched CNT-modified carbon microfiber	0.55^s	0–2.5×10^{-3s}	550^s	8	NR	NR	[41]
Ru and Rh NP/single carbon fiber	0.4	0–1.2×10^{-3}	48	10	5.9% (n = 3)	90%–35 measurem.	[42]
$SiO_2/SnO_2/Sb_2O_5$/MB graphite composite	−0.05	8.0×10^{-5}–9.0×10^{-4}	2.76	0.15	5% (n = 10)	90%–100 CV cycles	[43]
Titania sol–gel doped with MB/graphite electrode	−0.050	9.0×10^{-5}–2.3×10^{-3}	1.25×10^s	12	2% (n = 10)	88%–8 measurem.	[44]
Carbon black dispersion/SPCE	0.4**	0–2×10^{-4}	1.28×10^4	0.3	4% intraelect.; 13% interelect.	NR	[45]
LMC/GCE	0.25	2.5×10^{-5}–2.0×10^{-4}	8.86×10^3	0.2	NR	NR	[46]
OMC-PNR/GCE	0.7	0–1.6×10^{-3}	1.2×10^4	0.15	NR	NR	[47]
IL-graphene-chitosan/GCE	0.45	2.5×10^{-4}–2.0×10^{-3}	3.743×10^4 cm^{-2}	NR	NR	95.4%–10 min; 90%–30 min	[48]
GO/SPCEs	0.40	8.0×10^{-7}–5.0×10^{-4}	2.52×10^3	0.10	NR	96.7%–90 days at 4 °C	[49]
EGNs/GCE	0.32	2.0×10^{-6}–4.7×10^{-3}	5.35×10^5 cm^{-2}	NR	NR	92%–60 min	[50]
pTB/carbon felt	0.20	1–3×10^{-5}	3.18×10^5	0.3	NR	NR	[51]
PPS-SWCNT/EPPG	0.0	0–1.7×10^{-4}	5.76×10^5 cm^{-2}	0.01	NR	NR	[52]
SWCNT-HA/GCE	0.4	NR	6.86×10^3 cm^{-2}	63	9.2% (n = 3) batch to batch	95%–22 hs continuous operation	[53]
PEDOP/MWCNTs-Pd/GCE	0.42	1.0×10^{-6}–$1.3 \times 1\,0^{-2}$	1.27×10^4	0.18	1.64% (n = 10)	99%–20 days at 4 °C in 0.1 M PBS pH:7.4	[54]
PP–MWCNT/GCE	0.645	2.0×10^{-5}–8.0×10^{-4}	4.04×10^4 cm^{-2}	10	NR	NR	[55]
oxMWCNT-Chi/GCE	−0.05	1.0×10^{-5}–1.0×10^{-4}	(a) 3.2×10^3 cm^{-2}; (b) 1.2×10^4 cm^{-2}	(a) 4.0; (b) 2.0	NR	70%–1.5 hs continuous operation	[56]
AuNP–MWCNTs–Teflon composite	0.3 V	1.0×10^{-5}–1.0×10^{-4}	37.7	NR	37.7 (n = 10)	NR	[57]
MWCNT-PEI-Do/GCE	−0.025	1.0×10^{-5}–1.0×10^{-4}	1.9×10^4	3	8.9% (n = 15) intra and inter electrode and batch to batch	>90%–10 calibrations same surface equivalent to 3 hs continuous operation	This work

All oxidation potentials (E) are referred to Ag/AgCl reference electrode or converted to that potential if initially reported vs. other reference electrode.
Stability = Percentage of initial response after–"the stated condition"; NR = not reported; ^{S} = estimated from data shown when not stated in the paper; *DPV was used instead of amperometry; ** reported vs. Ag pseudo reference electrode; measurem = measurements; Cyt C:DOPE + UQ_{10}/poly-TTCA/AuNP/SPCE = Au nanoparticles electrodeposited on SPCE further covered with poly-5,20:50,200-terthiophene-30-carboxylic acid (poly-TTCA) modified with 1,2-dioleolyl-sn-glycero-3-phosphoethanolamine (DOPE), ubiquinone (UQ_{10}) and cytochrome c (Cyt C); SPCE = Screen printed carbon electrode; NADoxidase-Fc/SPCE = NAD oxidase and carboximethyl ferrocene (Fc) solution drop casted on SPCE; PEDOTSDS–AgNP–MB/GCE = GCE where modified potentiodynamically with poly(3,4-ethylene dioxythiophene-sodium dodecyl sulfate) [PEDOTSDS] + potentiostatically formed Ag nanoparticles (AgNP) + adsorption of MB; MB = Meldola's blue; $SiO_2/SnO_2/Sb_2O_5$/MB graphite composite = mixed oxide containing 25 wt% of SnO_2, coated with a thin layer of Sb_2O_5 chemically formed on the SiO_2/SnO_2 mixture and embedded with Meldola's Blue mixed with a graphite composite 60/40 (w/w); LMC/GCE = Large mesoporous carbons on GCE; OMC-PNR/GCE = potentiostatically polymerized poly(neutral red) (PNR) onto ordered mesoporous carbon (OMC) drop-coated on GCE; IL = ionic liquid; GO/SPCEs = SPCEs pre-oxidized at 1.9 V in 0.1 M PBS and drop-coated with Graphene Oxide (GO) dispersion; EGNs/GCE = exfoliated graphite (1 mg/mL in DMF) drop casted on GCE; pTB/carbon felt = electropolymerized poly(toluidine Blue) [pTB] on carbon felt; PPS-SWCNT/EPPG = poly(phenosafranin) [PPS] electropolymerized onto single wall carbon nanotubes [SWCNT] in DMF drop-casted onto edge-plane pyrolytic graphite [EPPG] electrode; SWCNT-HA/GCE = single-walled carbon nanotubes (SWCNT) dispersed in hyaluronic acid (HA) drop casted on GCE; PEDOP/MWCNTs-Pd/GCE = potentiodinamically polymerized 3,4-ethylenedioxypyrrole (PEDOP) on GCE drop casted with palladium-modified-multi-wall carbon nanotubes (MWCNTs-Pd); PP–MWCNT/GCE = diphenylalanine peptide (PP)-covered MWCNT dispersion drop casted on GCE; oxMWCNT-Chi/GCE = pre-oxidized MWCNT: water boiled (a) or microwaved in a concentrated nitric acid (70%) (b), dispersed in 0.01 W% Chitosan (Chi) solution drop casted on GCE; AuNP–MWCNTs–Teflon composite = colloidal gold (AuNP)–multi-walled carbon nanotubes (MWCNTs) composite electrode using Teflon as binding material.

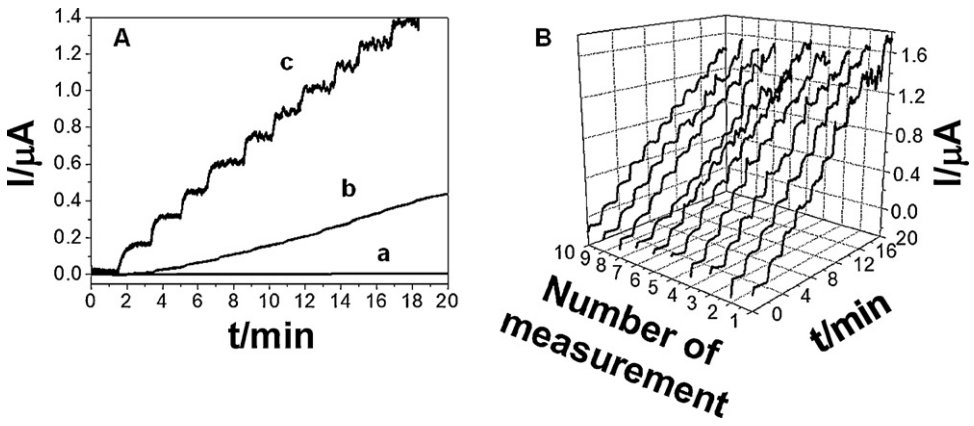

Fig. 8. Amperograms performed at −0.025 V for successive additions of 1.0×10^{-5} M, NADH comparing: (A) the first amperometric response between GCE (a), GCE/CNT-PEI (b) and GCE/CNT-PEI-Do surfaces (c); (B) 10 successive amperograms on the same GCE/CNT-PEI-Do surface.

the GCE/CNT-PEI-Do is $157 \pm 5\ \Omega$, demonstrating that this surface oxidation product acts as redox mediator for the electrooxidation of NADH.

3.4. Analytical applications of GCE/CNT-PEI-Do for NADH quantification

Hydrodymamic voltammograms (HDV) for a 2.0 mM NADH solution were performed to establish the working potential for further amperometric quantification. Fig. 7 shows a comparison between HDV obtained at different electrodes: GCE/CNT (a), GCE/CNT-PEI (b) and GCE/CNT-PEI-Do (c).

The improvement in the oxidation current obtained at the activated GCE/CNT-PEI-Do electrode is evident, since from potentials as negative as −0.100 V, the oxidation current is 3.5 and 8.0 times higher than those obtained at GCE/CNT and GCE/CNT-PEI, respectively. The maximum current difference between the three electrodes with a small relative error was obtained at −0.025 V. Therefore, −0.025 V was chosen as working potential for further amperometric studies.

Fig. 8A depicts typical amperograms obtained at −0.025 V at GCE (a), GCE/CNT-PEI (b) and activated GCE/CNT-PEI-Do (c), for successive additions of NADH. No response is observed at bare GCE, while at GCE/CNT-PEI, the signal is low and poorly defined due to the slow oxidation of NADH. On the contrary, at the activated GCE/CNT-PEI-Do, a clear, well defined and fast response is obtained after each addition of NADH. Excellent analytical parameters were obtained using this electrode as the relationship between oxidation current and NADH concentration is linear between 1.0×10^{-5} and 1.0×10^{-4} M with a sensitivity of $(19 \pm 2) \times 10^3\ \mu A\ M^{-1}$ (obtained from 15 electrodes prepared with 3 different dispersions), the detection limit is 3.0×10^{-6} M (taken as $3.3 \times \sigma/S$, where σ is the standard deviation of the blank signal and S is the sensitivity), and the quantification limit is 1.0×10^{-5} M (taken as $10 \times \sigma/S$).

One of the challenges when developing NADH electrochemical sensors is to obtain a design that makes possible successive determinations of NADH without passivation of the surface. Fig. 8B shows ten consecutive amperograms for NADH performed at −0.025 V using the same electrode surface. In all cases the response is clear and well defined. The difference in sensitivity between the first and the tenth calibration is just 12% ($17.7 \times 10^3\ \mu A\ M^{-1}$ vs. $15.6 \times 10^3\ \mu A\ M^{-1}$, respectively) without passivation by NADH oxidation products, demonstrating that the platform is robust, stable and reproducible.

Table 2 compares the analytical performances for the detection of NADH of our sensing platform and other sensors reported in the literature in the last two years (including diverse sensing platforms that are not directly comparable with ours since they use other electrode materials than polymer-modified MWCNTs). The related work previous to 2009 has already been extensively reviewed in literature [34,35] and therefore is not repeated here.

One of the main advantages of GCE/MWCNT-PEI-Do is that it allows the amperometric quantification of NADH at a low potential (−0,025 V) where most easily oxidizable interferents can be avoided. It is important to remark that among the results shown in Table 2, only four cases reported the NADH detection at negative potentials [40,43,44,56], but are less sensitive than our system. All other reported sensors used positive working potentials where other substances might interfere. Only few of them presented higher sensitivity [36,50–52], although they used other electrode materials like exfoliated graphite on GCE [50], carbon felt electrodes [51], or edge-plane pyrolytic graphite [52] which have higher surface area, and consequently, provide higher associated sensitivity. Comparing with other GCE or composite electrodes modified with MWCNT [55–57], the analytical performance of our system represents an improvement for NADH quantification since we can achieve better detection limits without additional doping-nanoparticles. Another important remark of our results is that we can accomplish at least 10 consecutive amperometric determinations, equivalent to 3 h of continuous operation of the same surface, which is not commonly achieved with other reported platforms. Only two groups have presented a similar stability at longer times [43,53]. This comparison clearly demonstrates that our sensor presents one of the most competitive performances, not only in terms of sensitivity and detection limits achieved, but also in terms of reproducibility, repeatability, long term stability of the surface and circumvention of potential interferents.

4. Conclusions

We can conclude that the covalent modification of PEI with Do has allowed: (i) to obtain a dispersing agent for CNT that confers better stability to the dispersion and mechanical strength to the deposit at GCE due to the π–π interaction of Do with the walls of CNT. (ii) To have a polymer modified with a redox marker that allows to follow the presence of CNT-PEI-Do, (iii) to have the precursor of the redox mediator that catalyzes the electrochemical reaction of NADH immobilized in the same dispersing agent. Therefore, PEI-Do is presented here as a very effective dispersing agent for CNT.

The modified electrode obtained with that dispersion, GCE/CNT-PEI-Do, gathers several properties: (i) the presence of PEI-Do greatly improves the mechanical resistance of the electrode, preventing any exfoliation of CNT to occur during measurements,

problem usually found in the case of GCE/CNT; (ii) the distribution of CNT deposits on the electrode surface is notably more homogeneous when the nanotubes are dispersed in PEI-Do compared to the dispersion in non-modified PEI.

The pretreatment of GCE/CNT-PEI-Do by cycling the potential between −0.200 and 0.400 V allows the formation of a redox couple able to catalyze the oxidation of NADH, permitting the sensitive quantification of NADH at potentials as low as −0.025 V without passivation of the electrode using the same surface for succesive amperometric detection of NADH.

The proposed sensing platform presents remarkable advantages such as high sensitivity, low detection limits, robustness, operation at low overpotentials, and highly stable electrochemical response without the common passivation of the surface by NADH oxidation products. Therefore, the electrode represents an interesting alternative for further developments of enzymatic biosensors based on NAD^+ mediation.

Acknowledgements

The authors thank CONICET, Ministerio de Ciencia y Tecnología de Córdoba, SECyT-UNC and ANPCyT for the financial support. A.G. and F.G. thanks CONICET for the fellowships. SEM images were taken in Laboratorio de Microscopía Electrónica y Análisis por Rayos X (LAMARX), Córdoba, Argentina.

References

[1] L. Gorton, E. Dominguez, in: A.J. Brad, M. Stratmann, G.S. Wilson (Eds.), Encyclopedia of Electrochemistry, Bioelectrochemistry, vol. 9, Wiley-VCH, Weinheim, 2002, pp. 67–143.
[2] M. Ates, A.S. Sarac, Prog. Org. Coat. 66 (2009) 337.
[3] B. Ge, Y. Tan, Q. Xie, M. Ma, S. Yao, Sens. Actuators B 137 (2009) 547.
[4] Z. Nazemi, E. Shams, M. KazemAmini, Electrochim. Acta 55 (2010) 7246.
[5] Y. Oztekina, Z. Yazicigil, A. Ramanaviciene, A. Ramanavicius, Sens. Actuators B 152 (2011) 37.
[6] M.D. Rubianes, M.C. Strumia, Electroanalysis 22 (2010) 1200.
[7] S. Kumar Vashist, D. Zheng, K. Al-Rubeaan, J.H.T. Luong, F. Shan Sheu, Biotechnol. Adv. 29 (2011) 169.
[8] B. Jacobs, M.J. rPeairs, B.J. Venton, Anal. Chim. Acta 662 (2010) 105.
[9] P. Cheng Ma, N. Siddiqui, G. Marom, J.K. Kima, Composit.: Part A 41 (2010) 1345.
[10] G. Dreselhaus, M.A. Pimenta, R. Saito, J.-C. Charlier, S.D.M. Brown, P. Corio, A. Marucci, M.S. Dresselhaus, in: Tomanek, Enbody (Eds.), Science and Applications of Nanotubes, Kluwer Academic, New York, 2000, pp. 275–295.
[11] M.F. Lin, D.S. Chuu, Phys. Rev. B: Condens. Matter Mater. Phys. 57 (1998) 10186.
[12] J. Wang, M. Musameh, Y. Lin, J. Am. Chem. Soc. 125 (2003) 2408.
[13] M. Zhang, A. Smith, W. Gorski, Anal. Chem. 74 (2002) 5039.
[14] A.K. Kaushik, P.R. Solanki, M.K. Pandey, K. Kaneto, S. Ahmad, B.D. Malhotra, Thin Solid Films 519 (2010) 1160.
[15] Y. Jalit, M.C. Rodríguez, M.D. Rubianes, S. Bollo, G.A. Rivas, Electroanalysis 20 (2008) 1623.
[16] M.C. Rodríguez, J. Sandoval, L. Galicia, S. Gutiérrez, G.A. Rivas, Sens. Actuators B 134 (2008) 559.
[17] S. Wang, D. Yu, L. Dai, J. Am. Chem. Soc. 133 (2011) 5182.
[18] A. Liu, I. Honma, M. Ichihara, H. Zhon, Nanotechnology 17 (2006) 2845.
[19] F. Gutiérrez, G. Ortega, J.L. Cabrera, M.D. Rubianes, G.A. Rivas, Electroanalysis 22 (2010) 2650.
[20] J. Filip, J. Sefcovicová, P. Tomcik, P. Gemeiner, J. Tkac, Talanta 84 (2011) 355.
[21] M.D. Rubianes, G.A. Rivas, Electrochem. Commun. 9 (2007) 480.
[22] M.C. Rodríguez, M.D. Rubianes, G.A. Rivas, J. Nanosci. Nanotechnol. 8 (2008) 6003.
[23] A. Sánchez Arribas, E. Bermejo, M. Chicharro, A. Zapardiel, G.L. Luque, N.F. Ferreyra, G.A. Rivas, Anal. Chim. Acta 596 (2007) 183.
[24] S. Meuer, L. Braun, R. Zentel, ChemPhys. 210 (2009) 1528.
[25] Y. Zhang, L. Liu, F. Xi, T. Wu, X. Lin, Electroanalysis 22 (2010) 277.
[26] Ch. Xiao, X. Chu, B. Wu, H. Pang, X. Zhang, J. Chen, Talanta 80 (2010) 1719.
[27] N. Nakashima, Sci. Technol. Adv. Mater. 7 (2006) 609.
[28] A.S. Kumar, P. Swetha, Colloids Surf. A: Physicochem. Eng. Aspects 384 (2011) 597.
[29] O. Segut, G. Herlem, B. Lakard, V. Blondeau-Patissier, M. Nardin, S. Gree, J.Y. Rauch, Synth. Met. 160 (2010) 1359.
[30] D.C.S. Tse, T. Kuwana, Anal. Chem. 50 (1978) 1315.
[31] A. Brun, R. Rosset, Electroanal. Chem. Interfac. Electrochem. 49 (1974) 287.
[32] T.M. Nahir, Langmuir 18 (2002) 5283.
[33] D.S. Campbell-Rance, T.T. Doan, M.C. Leopold, J. Electroanal. Chem. 662 (2011) 343.
[34] A. Radoi, D. Compagnone, Bioelectrochemistry 76 (2009) 126.
[35] S.A. Kumar, S.M. Chen, Sensors 8 (2008) 739.
[36] Y. Li, L. Shi, W. Ma, D.-W. Li, H.-B. Kraatz, Y.-T. Long, Bioelectrochemistry 80 (2011) 128.
[37] D.G. Dilgina, D. Gligor, H.I. Gökçel, Z. Dursunb, Y. Dilgin, Biosens. Bioelectron. 26 (2010) 411.
[38] K.-S. Lee, M.-S. Won, H.-B. Noh, Y.-B. Shim, Biomaterials 31 (2010) 7827.
[39] C. Creanga, N. El Murr, J. Electroanal. Chem. 656 (2011) 179.
[40] A. Balamurugan, K.-C. Ho, S.-M. Chen, T.-Y. Huang, Colloids Surf. A: Physicochem. Eng. Aspects 362 (2010) 1.
[41] X. Zhao, X. Lu, W.T.Y. Tze, P. Wang, Biosens. Bioelectron. 25 (2010) 2343.
[42] S. Poorahong, P. Santhosh, G. Valdés Ramírez, T.-F. Tseng, J.I. Wong, P. Kanatharana, P. Thavarungkul, J. Wang, Biosens. Bioelectron. 26 (2011) 3670.
[43] T.C. Canevari, R.C.G. Vinhas, R. Landers, Y. Gushikem, Biosens. Bioelectron. 26 (2011) 2402.
[44] J. Adamski, J. Kochana, Cent. Eur. J. Chem. 9 (2011) 185.
[45] F. Arduini, A. Amine, C. Majorani, F. Di Giorgio, D. De Felicis, F. Cataldo, D. Moscone, G. Palleschi, Electrochem. Commun. 12 (2010) 346.
[46] J. Bai, B. Lu, X. Bo, L. Guo, Electrochem. Commun. 12 (2010) 1563.
[47] B. Lu, J. Bai, X. Bo, L. Yang, L. Guo, Electrochim. Acta 55 (2010) 4647.
[48] C. Shan, H. Yang, D. Han, Q. Zhang, A. Ivaska, L. Niu, Biosens. Bioelectron. 25 (2010) 1504.
[49] L. Zhang, Y. Li, L. Zhang, D.-W. Li, D. Karpuzov, Y.-T. Long, Int. J. Electrochem. Sci. 6 (2011) 819.
[50] J. Zhu, X. Chen, Wensheng Yang, Sens. Actuators B 150 (2010) 564.
[51] Y. Hasebe, Y. Wang, K. Fuk, J. Environ. Sci. 23 (6) (2011) 1050.
[52] F.S. Saleh, T. Okajima, F. Kitamura, L. Mao, T. Ohsaka, Electrochim. Acta 56 (2011) 4916.
[53] J. Filip, P. Jana Šefèovièová, P. Tomèik, J. Gemeiner, J. Tkac, Talanta 84 (2011) 355.
[54] J.-M. You, S. Jeon, Electrochim. Acta 56 (2011) 10077.
[55] J. Yuan, J. Chen, X. Wu, K. Fang, L. Niu, J. Electroanal. Chem. 656 (2011) 120.
[56] M. Wooten, W. Gorski, Anal. Chem. 82 (2010) 1299.
[57] J. Manso, M. Mena, P.Y. Sedeno, J.M. Pingarron, Electrochim. Acta 53 (2008) 4007.